Paper Number:
DOE/MC/28055-97/C0840

Title:
Recent Progress in Tubular Solid Oxide Fuel Cell Technology

Authors:
S.C. Singhal

Contractor:
Westinghouse Science & Technology Center
1310 Beulah Road
Pittsburgh, PA 15235-5098

Contract Number:
DE-FC21-91MC28055

Conference:
Fifth International Symposium on Solid Oxide Fuel Cells

Conference Location:
Aachen, Germany

Conference Dates:
June 2-5, 1997

Conference Sponsor:
Electrochemical Society (USA), International Society of Electrochemistry

Disclaimer

DOE/MC/28055--97/C0840
CONF-9706108--

RECENT PROGRESS IN TUBULAR SOLID OXIDE FUEL CELL TECHNOLOGY

S.C. Singhal

Westinghouse Electric Corporation
Science & Technology Center
1310 Beulah Road
Pittsburgh, PA 15235, USA

ABSTRACT

The tubular design of solid oxide fuel cells (SOFCs) and the materials used therein have been validated by successful, continuous electrical testing over 69,000 h of early technology cells built on a calcia-stabilized zirconia porous support tube (PST). In the latest technology cells, the PST has been eliminated and replaced by a doped lanthanum manganite air electrode tube. These air electrode supported (AES) cells have shown a power density increase of about 33% with a significantly improved performance stability over the previously used PST type cells. These cells have also demonstrated the ability to thermally cycle over 100 times without any mechanical damage or performance loss. In addition, recent changes in processes used to fabricate these cells have resulted in significant cost reduction. This paper reviews the fabrication and performance of the state-of-the-art AES tubular cells. It also describes the materials and processing studies that are underway to further reduce the cell cost, and summarizes the recently built power generation systems that employed state-of-the-art AES cells.

1. INTRODUCTION

High temperature solid oxide fuel cells (SOFCs) offer a clean, pollution-free technology to electrochemically generate electricity at high efficiencies. These fuel cells provide high efficiency, reliability, modularity, fuel adaptability, and very low levels of NO_x and SO_x emissions. Quiet, vibration-free operation of solid oxide fuel cells also eliminates noise usually associated with conventional power generation systems. Furthermore, because of their high temperature of operation (~1000°C), these cells can be operated directly on natural gas eliminating the need for an expensive, external reformer system. These fuel cells also produce high quality exhaust heat which can be used for process heat or a bottoming electric power cycle to further increase the overall efficiency. Also, pressurized SOFCs can be successfully

used as replacements for combustors in combustion turbines; such integrated SOFC-combustion turbine power systems are expected to reach efficiencies approaching 70%.

In the early technology tubular solid oxide fuel cells, the active cell components were deposited in the form of thin layers on a calcia-stabilized zirconia porous support tube (PST). The materials and fabrication processes for these PST cells have been described previously (*1-4*). The tubular design of SOFCs and the materials used therein have been validated by successful electrical testing of these early PST cells over an extended period. The voltage output of such a cell over 69,000 h is plotted in Fig. 1, which shows a degradation rate of less than 0.5% per 1,000 h. In the state-of-the-art cells, the calcia-stabilized zirconia support tube has been completely eliminated and replaced by a doped lanthanum manganite tube. These latest technology tubular cells are designated as air electrode supported (AES) cells. This paper reviews the fabrication processes and performance of these AES cells, and summarizes the power generation systems that employed such cells.

2. STATE-OF-THE-ART AIR ELECTRODE SUPPORTED CELLS

In the state-of-the-art air electrode supported cells, a doped lanthanum manganite tube is used. This tube is extruded and sintered to about 30 to 35 porosity, and serves as the air electrode on to which the other cell components are fabricated in thin layer form. Schematic design of such a cell is shown in Fig. 2. The active length of the cells has also been increased to increase the power output per cell. A greater cell power output decreases the number of cells required in a given power size generator and thus improves SOFC power plant economics. The active length for today's commercial prototype AES cells is 150 cm. Additionally, the diameter of the tube in longer length AES cells has been increased to 2.2 cm to accommodate larger pressure drops encountered in longer length cells. Fig. 3 shows the power output from different cells illustrating the many-fold increase in power output from the latest technology AES cells.

The fabrication of PST cells involved three electrochemical vapor deposition (EVD) steps, one each for the doped $LaCrO_3$ interconnection, the yttria-stabilized zirconia (YSZ) electrolyte, and the Ni-YSZ fuel electrode. Though EVD provides very high quality thin films (*5,6*), it requires capital intensive equipment making the process rather expensive. Investigations on alternate processing techniques have been underway at Westinghouse for several years to replace one or more EVD steps with a more cost-effective approach. The interconnection is now deposited by plasma spraying calcium aluminate containing lanthanum chromite powder over porous, doped lanthanum manganite air electrode tube; calcium aluminate facilitates densification during plasma spraying and subsequent heat treatment (*7*). The plasma

sprayed interconnections are single phase, perovskite structure. These interconnections have a thermal expansion coefficient much better matched to that of the electrolyte than the previously-used EVD Mg-doped lanthanum chromite interconnection. Plasma spraying of interconnections has now been implemented in the manufacturing of all AES SOFCs. This has resulted in reduced process cycle time, increased yield, and a major reduction in cell fabrication cost. Plasma spraying will allow continuous, fully automated deposition of interconnection films in commercial SOFC production. A representative micrograph of the plasma sprayed interconnection is shown in Fig. 4, which shows the interconnection to be uniform in thickness and dense with no open porosity. The materials and fabrication processes for the state-of-the-art AES cells are summarized in Table I.

Table I. Materials and Fabrication Processes for State-of-the-Art AES Cells.

Component	Material	Thickness	Fabrication Process
Air Electrode Tube	Doped $LaMnO_3$	2.2 mm	Extrusion-sintering
Electrolyte	$ZrO_2(Y_2O_3)$	40 μm	Electrochemical vapor deposition
Interconnection	Doped $LaCrO_3$	85 μm	Plasma spraying
Fuel Electrode	Ni-$ZrO_2(Y_2O_3)$	100 μm	Slurry spray-electrochemical vapor deposition

3. CELL OPERATION AND PERFORMANCE

A large number of AES cells with plasma sprayed interconnections have been electrically tested for up to about 13,000 h. These cells have shown the ability to perform for extended periods of time under a variety of operating conditions with little performance degradation. The performance degradation has decreased from about 0.5% per 1,000 h for PST cells to less than 0.2% per 1,000 h for AES cells. The voltage-current characteristics of the AES cells (1.56 cm diameter, 50 cm active length) at 900, 950, and 1000°C, with 89% H_2 + 11% H_2O fuel (85% fuel utilization) and air as oxidant (4 stoichs) are shown in Fig. 5. The power density of these AES cells is about 33% greater than that of previously used PST cells.

In addition to improved performance, the AES SOFCs have shown the ability to thermally cycle to room temperature over 100 times without any mechanical damage or performance loss as shown in Fig. 6. This ability to sustain thermal cycles is essential for any SOFC generator to be commercially viable. In addition to the

ability to sustain large number of thermal cycles, the cells can be cycled with a rapid temperature ramp rate making SOFC generators suitable for rapid start-up or restart following a power interruption. The thermal cycles in Fig. 6 are for temperature ramps from ambient temperature to 1000°C within 5 h or less. This ramp rate of 200°C/h would allow a generator to move from a hot standby condition at 600°C to full power at 1000°C within 2 h.

Westinghouse in conjunction with Ontario Hydro Technologies has also tested AES cells at pressures up to 15 atmospheres on both hydrogen and natural gas fuels. Fig. 7 shows the comparative voltage-current density curves and Fig. 8 the power output curves at 1, 3, 5, 10 and 15 atm for a 2.2 cm diameter, 150 cm active length AES cell at 1000°C. Operation at elevated pressures yields a higher cell voltage at any current density due to increased Nernst potential and reduced cathode polarization, and thereby permits higher stack efficiency and greater power output. With pressurized operation, SOFCs can be successfully used as replacements for combustors in combustion turbines; such integrated SOFC-combustion turbine power systems are expected to reach efficiencies approaching 70%, and thus result in reduced fuel consumption cost and reduced capital cost per unit power output (*8,9*).

4. INVESTIGATIONS IN PROGRESS TO FURTHER REDUCE CELL COST

Elimination of one of the cell components (calcia-stabilized zirconia support tube) and replacement of one EVD step by plasma spraying (for depositing interconnection) has resulted in a major reduction in the cost of the AES cells and the cost of electricity ($/kW) produced by using such cells. Investigations are underway to further reduce the cost of these cells by reducing the cost of materials used in SOFCs and replacing remaining EVD steps by a more cost-effective sintering approach.

Over 90% of the weight of a tubular AES cell is that of the doped lanthanum manganite air electrode tube. Presently, the air electrode material is synthesized using high purity component oxides such as La_2O_3 and MnO_2. Over 70% reduction in the cost of air electrode raw materials is possible if mixed lanthanides are used instead of pure lanthanum compounds to synthesize the air electrode powder. These mixed lanthanides contain Nd, Pr, Ce and Sm in addition to La. AES cells have now been fabricated using air electrode powder synthesized using mixed lanthanides. Fig. 9 compares the performance of a cell fabricated using mixed lanthanides for the air electrode to that of a cell fabricated using pure lanthanum oxide instead. The performance of the cell with air electrode fabricated using mixed lanthanides at 400 mA/cm^2 is only about 8% lower, primarily due to slightly higher resistivity of the mixed lanthanides air electrode and non-optimized cell fabrication conditions. Further adjustments in the composition of the air electrode material synthesized using mixed

lanthanides are expected to result in lower air electrode resistivity and a cell performance equivalent to that of cells using high purity air electrode material synthesized using pure lanthanum oxide. The substitution of mixed lanthanides for lanthanum in air electrodes results in a major reduction in the cost of materials used in the manufacture of tubular SOFCs.

Investigations to deposit Ni-YSZ fuel electrode by a non-EVD process have also been successful. Deposition of a Ni-YSZ slurry over the YSZ electrolyte followed by sintering has yielded fuel electrodes that are equivalent in electrical conductivity to those fabricated by the EVD process. Cells fabricated with only one-EVD step (plasma sprayed interconnection, EVD electrolyte, and sintered fuel electrode) have shown electrical performance equivalent to those of the two-EVD steps (plasma sprayed interconnection, EVD electrolyte, and EVD fuel electrode) cells. Fig. 10 shows the voltage vs. time and Fig. 11 the voltage-current characteristics of a one-EVD step cell and a two-EVD steps cell. Both cells were operated at 1000°C on 89% H_2 + 11% H_2O fuel at 85% fuel utilization. Even at this high fuel utilization, the performance of the cell with sintered fuel electrode is comparable to that of the cell with the EVD fuel electrode. In fact, the sintered fuel electrode polarization is even lower than the already very low (7-15 mV) EVD fuel electrode polarization. This is believed to be due to a larger contact area and a greater number of electrochemically active sites at the electrolyte/sintered fuel electrode interface; a representative micrograph of the sintered fuel electrode is shown in Fig. 12. This fuel electrode sintering process is currently being scaled up for cell manufacturing.

In the very near future, the AES cell production process will use EVD for only the electrolyte. The EVD process deposits very thin (20 to 40 μm thick), gas-tight electrolyte film over the porous air electrode, reliably, uniformly, and in acceptable cycle time. Nonetheless, deposition of the YSZ electrolyte film by a non-EVD technique such as colloidal/electrophoretic deposition of YSZ over porous air electrode tube followed by sintering is also being investigated. If successful, this will result in further reduction in the cost of manufacturing SOFCs.

5. SOFC POWER GENERATION SYSTEMS WITH AES CELLS

Since 1984, Westinghouse has designed, built, and tested successively larger-size SOFC power generation systems using PST type cells. The design and operation of these systems have been described previously (*1,2*). Recently, two 25 kW systems, each consisting of 576 50-cm active length AES cells (with EVD electrolyte, EVD fuel electrode, and plasma sprayed interconnection), were built. One system was operated at the Southern California Edison Company's Highgrove Generating Station in Grand Terrace (near San Bernardino), California, under a program with the U.S.

Department of Defense's Advanced Research Projects Agency (ARPA). In addition to the SOFC generator, this system also consisted of a logistic fuel processor, located external to the SOFC stack, enabling the system to operate on either natural gas or on reformate from a logistic fuel (DF-2 diesel or JP-8 jet turbine fuel). This system was successfully operated for 5,582 h before the project completion; 766 h on jet turbine fuel, 1,555 h on diesel fuel, and 3,261 h on natural gas. During this time, the system endured five thermal cycles to room temperature, produced up to 27 kW on each of the three fuels, and showed no evidence of performance degradation.

The other system, built for a consortium of Osaka Gas and Tokyo Gas, is still under operation and has passed 12,400 h (as of January 1, 1997) of successful operation on desulfurized natural gas without any sign of performance degradation. During this period, the unit has achieved 25 kW of power output and has endured eight thermal cycles to ambient temperature.

A 100 kW SOFC power generation system is presently being built for delivery in 1997 to a consortium of Dutch and Danish utilities (EDB/ELSAM). The system will be installed and operated at Duiven (near Arnhem), The Netherlands, at a district heating system owned by NUON, one of the group of five Dutch gas and electricity distribution utilities which belong to the EDB consortium. The system employs 1,152 state-of-the-art AES cells with plasma sprayed interconnections (2.2 cm diameter, 150 cm active length); these cells are prototypic of the cells that are planned to be used in MW-class commercial SOFC generators. The system will deliver 100 kW net ac to the grid at an overall thermal efficiency of 50% (ac/LHV) and recover 25% of the fuel energy in hot water yielding a total fuel effectiveness (at 100 kW ac) of 75%. The maximum power output of the system is 160 kW net ac; at maximum power, the fuel effectiveness of the system will approach 80%.

All the systems described above have been or will be operated at 1 atm pressure. Plans to design, build, and test integrated pressurized SOFC-combustion turbine power generation systems in the 250 kW to integer MW sizes are presently being finalized.

6. SUMMARY

State-of-the-art air electrode supported SOFCs have exhibited significant improvements in performance, reliability, and ability to sustain thermal cycles, over previous tubular designs. This has been confirmed by successful operation of two 25 kW power generation systems employing such cells. In addition, very significant cost reductions have been achieved by adopting non-EVD processes in cell production; further reductions in materials and processing costs will be realized when

the programs currently underway are proven successful and are implemented in cell manufacturing.

ACKNOWLEDGMENTS

The author acknowledges the contributions of his many colleagues whose work is reviewed in this paper. The development of the SOFC technology has been supported by the U.S. Department of Energy (DOE), the Gas Research Institute (GRI), and various utility and commercial sources. The pressurized SOFC testing effort is supported by Ontario Hydro Technologies and their Canadian funding partners, and New Energy Development Organization (NEDO) of Japan and its participating electric power companies.

REFERENCES

1. S. C. Singhal, "Recent Progress in Zirconia-Based Fuel Cells," in Proceedings of the Fifth International Conference on the Science and Technology of Zirconia, (S. P. S. Badwal, M. J. Bannister, and R. H. J. Hannink, eds.), Technomic Publishing Company, Lancaster, PA, (1993), pp. 631-651.

2. S. C. Singhal, "Tubular Solid Oxide Fuel Cells, in Proceedings of the Third International Symposium on Solid Oxide Fuel Cells, (S. C. Singhal and H. Iwahara, eds.), The Electrochemical Society, Inc., Pennington, NJ, Vol. 93-4, (1993), pp. 665-677.

3. S. C. Singhal, "Advances in Tubular Solid Oxide Fuel Cell Technology," in Proceedings of the Fourth International Symposium on Solid Oxide Fuel Cells, (M. Dokiya, O. Yamamoto, H. Tagawa, and S. C. Singhal, eds.), The Electrochemical Society, Inc., Pennington, NJ, Vol. 95-1, (1995), pp. 195-205.

4. S. C. Singhal, "Status of Solid Oxide Fuel Cell Technology," in Proceedings of the 17th Risø International Symposium on Materials Science: High Temperature Electrochemistry - Ceramics and Metals (F. W. Poulson, N. Bonanos, S. Linderoth, M. Mogensen, and B. Zachau-Christiansen, eds.), Risø National Laboratory, Roskilde, Denmark, (1996), pp. 123-138.

5. U. B. Pal and S. C. Singhal, "Electrochemical Vapor Deposition of Yttria-Stabilized Zirconia Films," J. Electrochem. Soc., Vol. 137, (1990), pp. 2937-2941.

6. U. B. Pal and S. C. Singhal, "Growth of Perovskite Films by Electrochemical Vapor Deposition," High Temp. Science, Vol. 27, (1990), pp. 251-264.

7. L. H. Kuo, S. D. Vora, and S. C. Singhal, "Plasma Spraying of Lanthanum Chromite Films for Solid Oxide Fuel Cell Interconnection Application," J. Amer. Ceram. Soc., Vol. 80, (1997), in press.

8. W. G. Parker and F. P. Bevc, "SureCELL™ Integrated Solid Oxide Fuel Cell/Combustion Turbine Power Plants for Distributed Power Applications," in Proceedings of the 2nd International Fuel Cell Conference, New Energy and Industrial Technology Development Organization, Kobe, Japan, (1996), pp. 275-278.

9. S. E. Veyo and W. Lundberg, "Tubular SOFC and SOFC/Gas Turbine Combined Cycles-Status and Prospects," in Fuel Cell Seminar Abstracts, Courtesy Associates, Inc., Washington, DC, (1996), pp. 776-779.

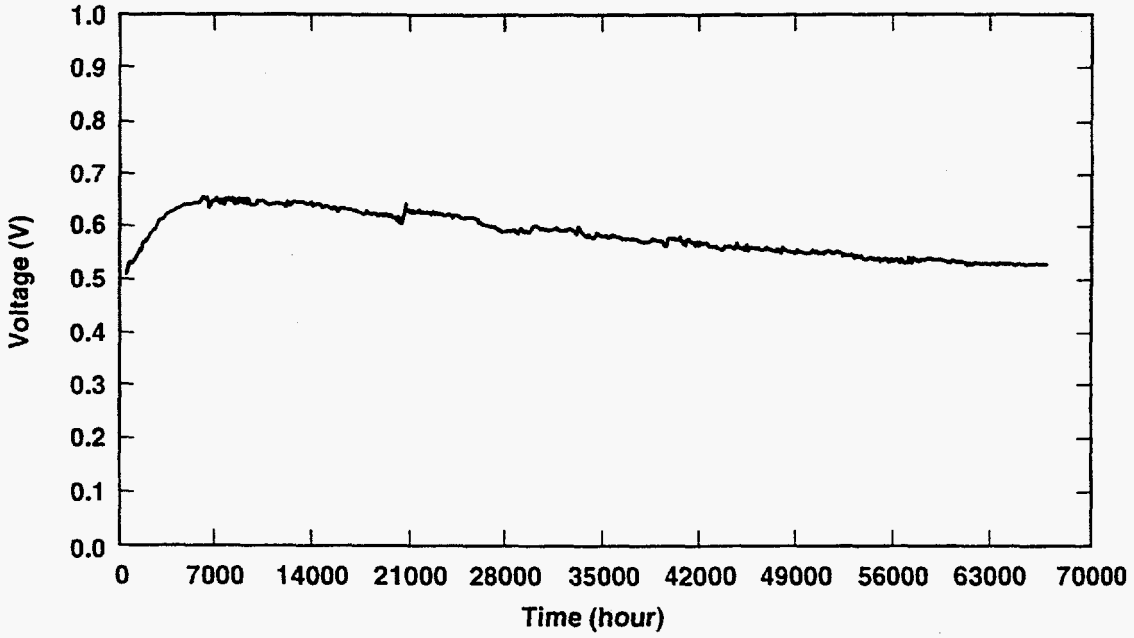

Fig. 1. Long term test of an early-technology PST cell.

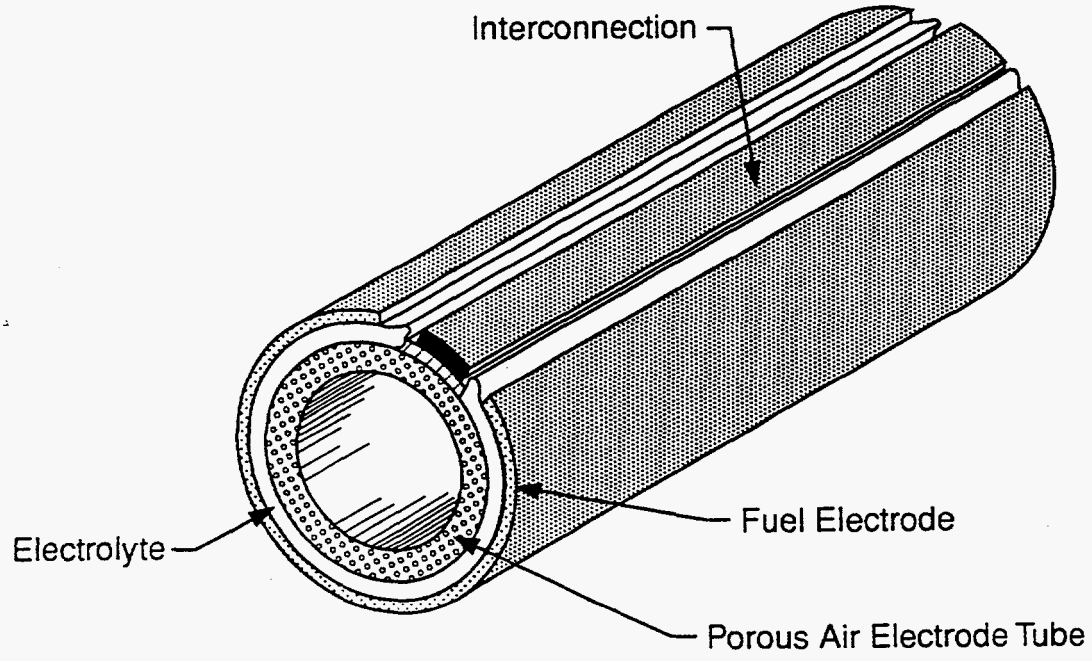

Fig. 2. Air electrode supported (AES) type tubular solid oxide fuel cell design.

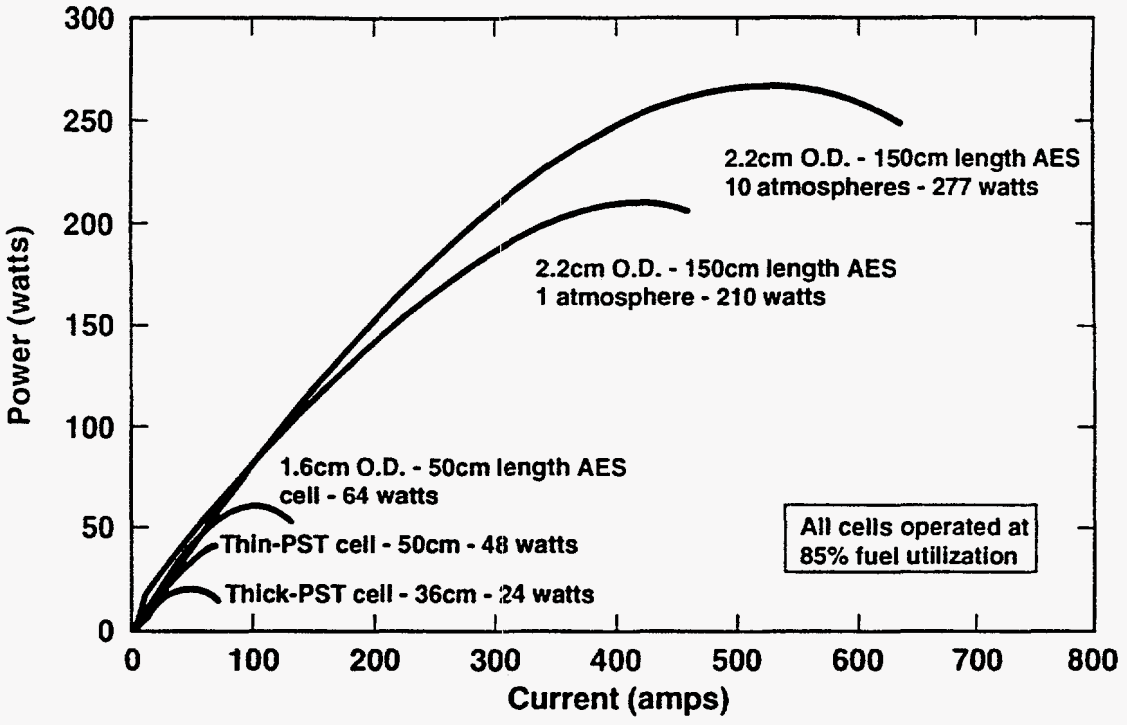

Fig. 3. Power output of different type and length cells.

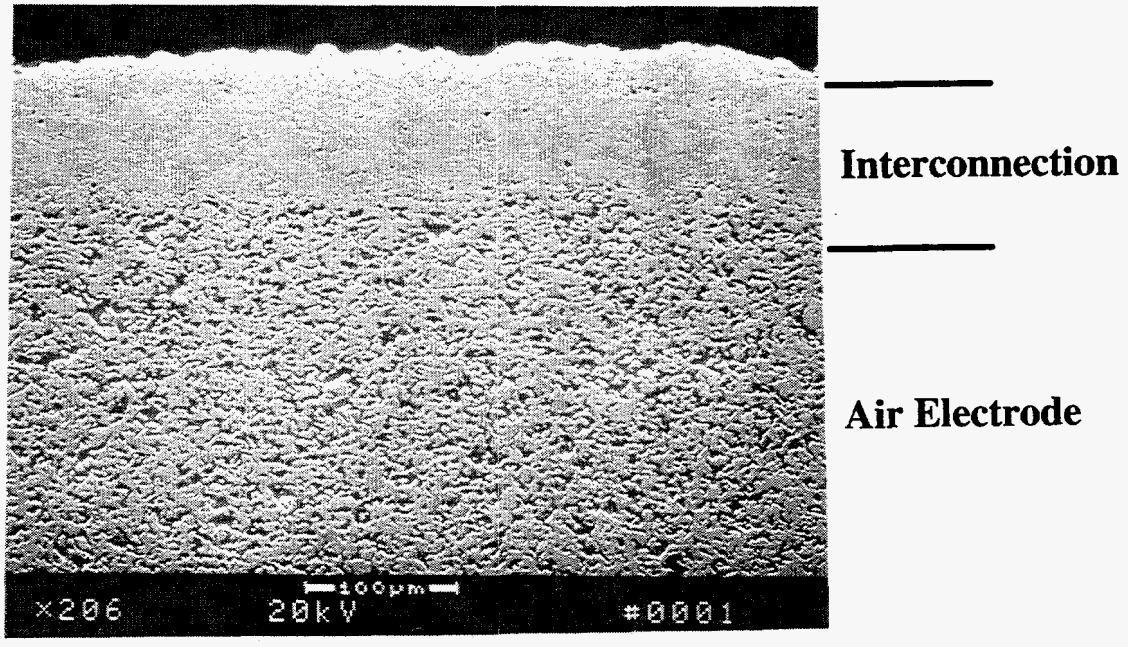

Fig. 4. Representative micrograph of the plasma sprayed interconnection over air electrode.

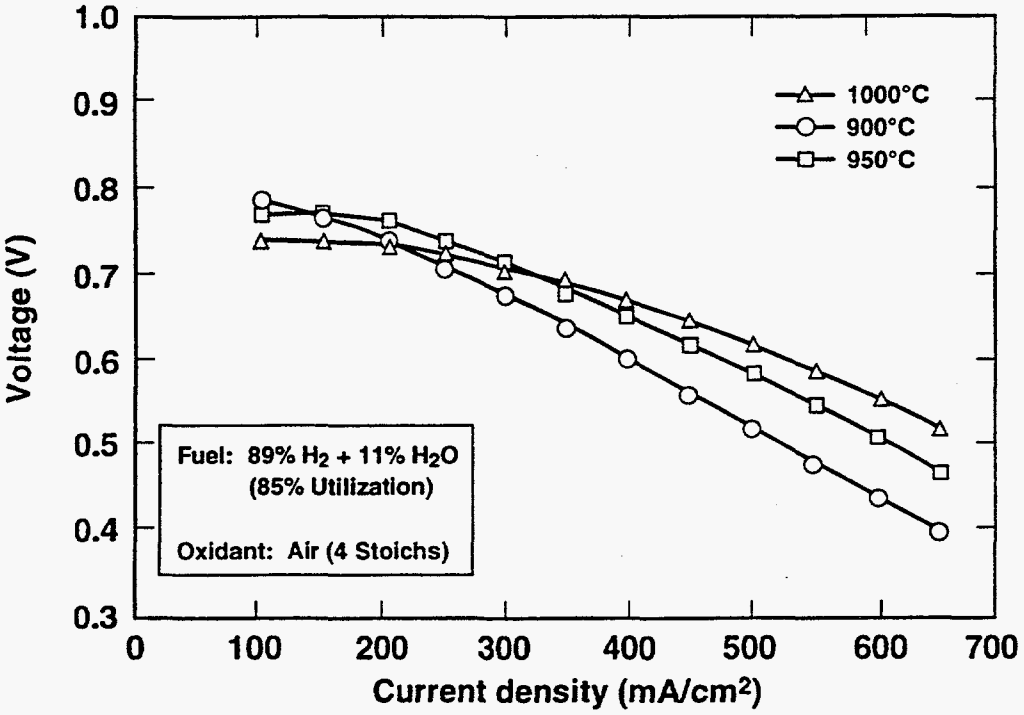

Fig. 5. Voltage-current characteristics of an AES cell at different temperatures.

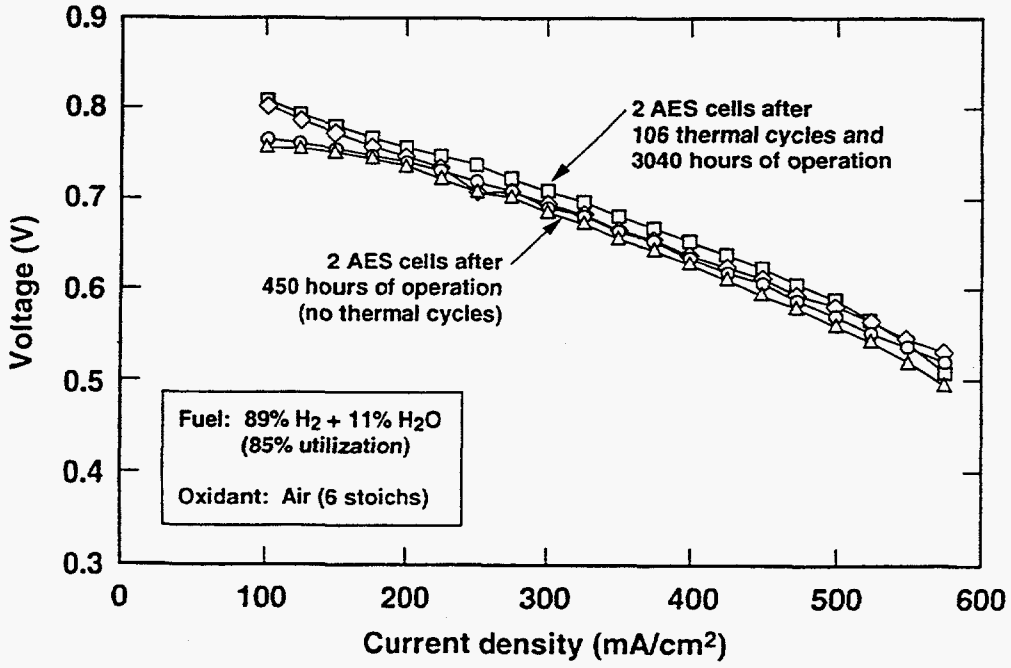

Fig. 6. Thermal cycling capability of AES cells.

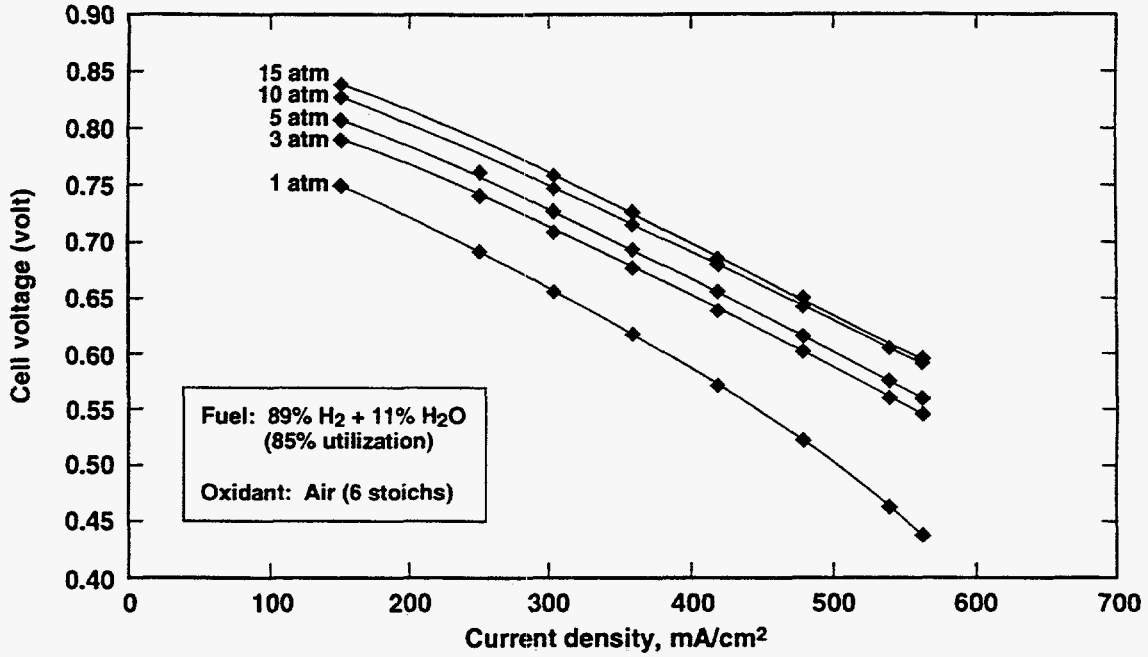

Fig. 7. Effect of pressure on AES cell performance at 1000°C.

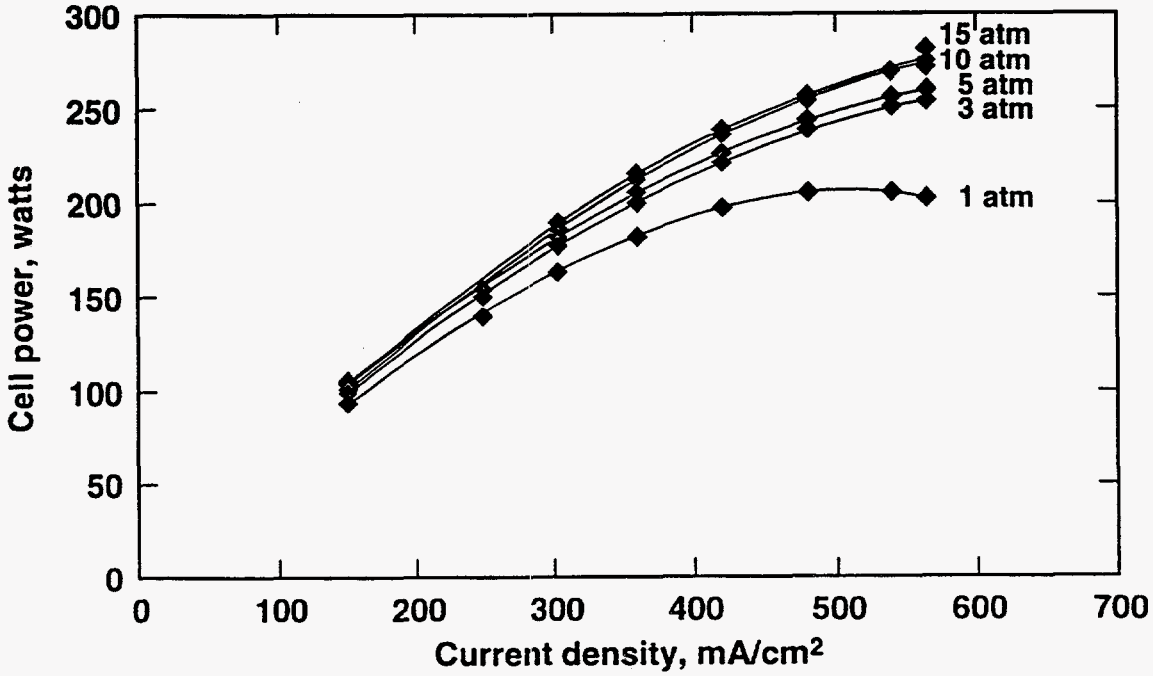

Fig. 8. Power output of an AES cell at 1000°C as a function of pressure.

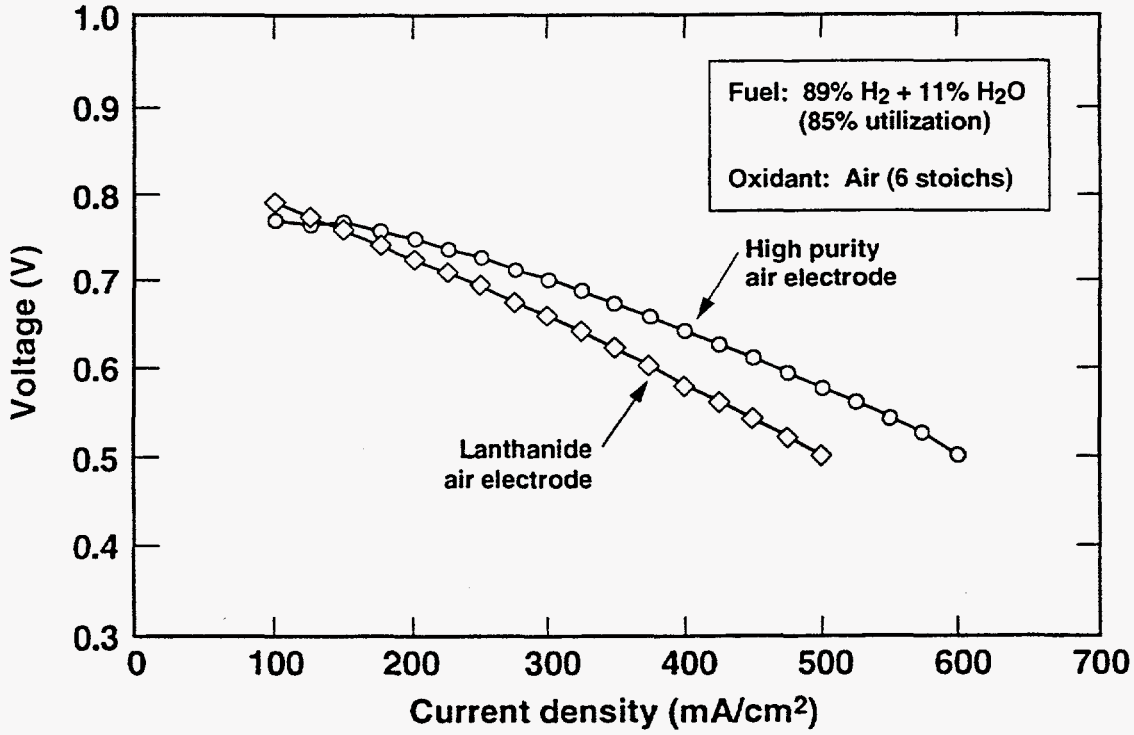

Fig. 9. Effect of air electrode material purity on the voltage-current characteristics of AES cells at 1000°C.

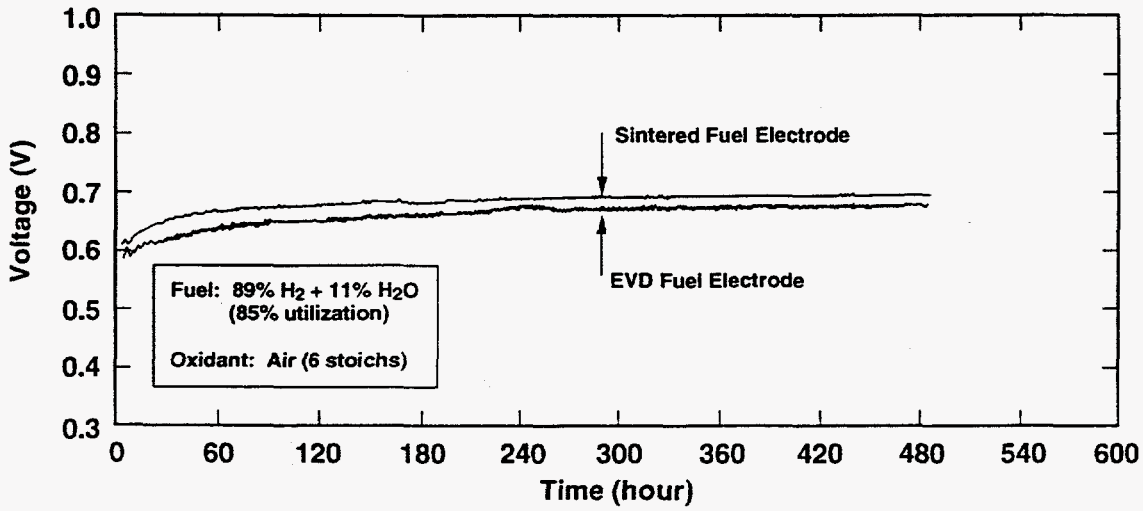

Fig. 10. Relative performance of the EVD and the sintered fuel electrodes at 1000°C and 313 mA/cm^2.

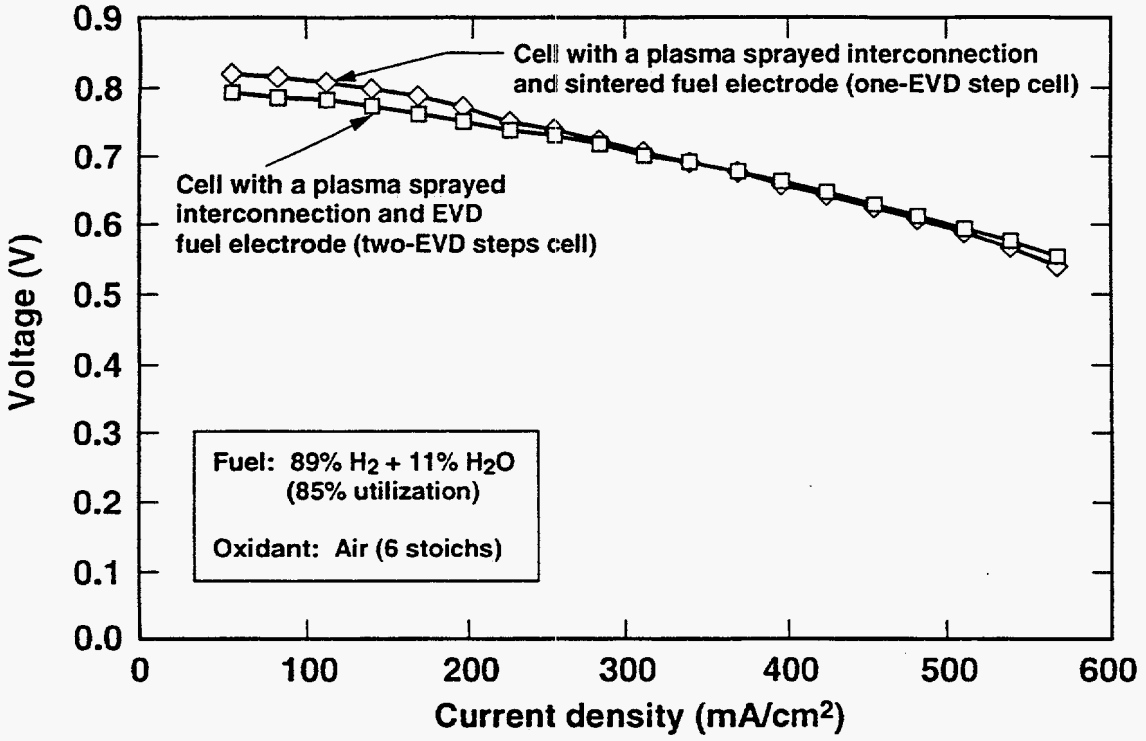

Fig. 11. A comparison of the voltage-current characteristics of the one-EVD step and the two-EVD step cells at 1000°C.

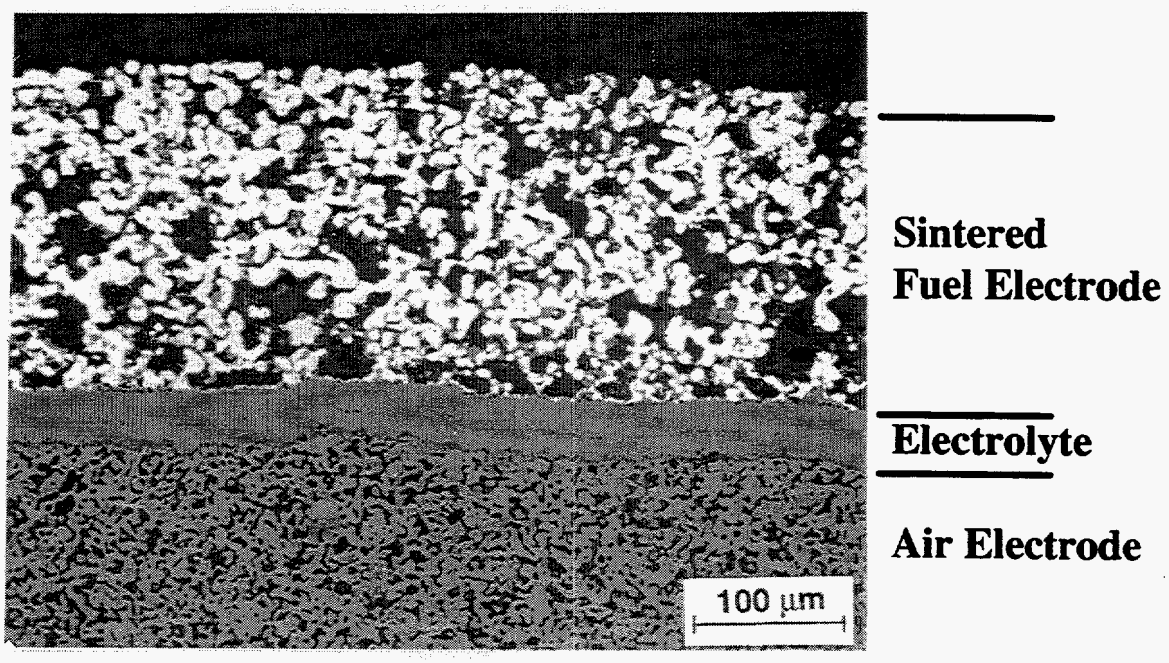

Fig. 12. Representative micrograph of a sintered fuel electrode.